# Light Energy Conversion Using Mixed Molecular Nanoclusters. Porphyrin and $C_{60}$ Cluster Films for Efficient Photocurrent Generation

**Taku Hasobe,[†,‡] Hiroshi Imahori,[*,§,||] Shunichi Fukuzumi,[*,‡] and Prashant V. Kamat[*,†]**

*Notre Dame Radiation Laboratory, University of Notre Dame, Notre Dame, Indiana 46556-0579, Department of Material and Life Science, Graduate School of Engineering, Osaka University, CREST, Japan Science and Technology Agency (JST), Suita, Osaka 565-0871, Japan, Department of Molecular Engineering, Graduate School of Engineering, Kyoto University, PRESTO, Japan Science and Technology Agency (JST), Katsura, Nishikyo-ku, Kyoto 615-8510, Japan, and Fukui Institute for Fundamental Chemistry, Kyoto University, 34-4, Takano-Nishihiraki-cho, Sakyo-ku, Kyoto 606-8103, Japan*

*Received: June 29, 2003; In Final Form: August 22, 2003*

Composite molecular nanoclusters of fullerene and porphyrin prepared in acetonitrile/toluene mixed solvent absorb light over the entire spectrum of visible light. Upon slow evaporation of the solvent on the copper grid, these mixed nanoclusters undergo close-packed stacking to produce either tubular- or square-shaped microcrystallites and differ from those obtained from single-component clusters. The highly colored composite clusters can be assembled as 3-dimensional arrays onto nanostructured $SnO_2$ films using an electrophoretic deposition approach. The composite cluster films exhibit an incident photon-to-photocurrent efficiency (IPCE) as high as 17% at an applied potential of 0.2 V vs SCE, which is significantly higher than the additive effect observed from either porphyrin (IPCE = 1.6%) or fullerene clusters (IPCE = 5.0%) under similar photoelectrochemical conditions. The high IPCE values observed with porphyrin and $C_{60}$ clusters demonstrate the synergy of these systems toward yielding efficient photoinduced charge separation within these composite nanoclusters.

## Introduction

The requirement to develop inexpensive renewable energy sources has stimulated new approaches for production of efficient, low-cost photovoltaic devices.[1−5] The construction of efficient photovoltaic devices requires an enhanced light-harvesting efficiency of chromophore molecules throughout the solar spectrum together with a highly efficient conversion of the harvested light into electrical energy.[1−5] Nanostructured semiconductor metal oxide films have been widely utilized as photoelectrochemical solar cells.

In recent years attention has been drawn toward developing heterojunction organic solar cells, which possess an active layer of a conjugated donor polymer and an acceptor fullerene.[6] In these polymer blends, efficient photoinduced electron transfer occurs at the donor−acceptor interface, and intimate mixing of donor and acceptor is therefore beneficial for efficient charge separation.[6] For efficient transport of the positive charge carriers through the donor phase and of electrons via the acceptor phase to the electrodes, a phase-segregated bicontinuous network is required.[6] Little attention has been given to utilizing other organic systems for photocurrent generation.

Fullerenes hold a great promise as a spherical electron acceptor on account of their small reorganization energy in electron-transfer reactions.[7,8] Porphyrins, on the other hand, used as an electron donor as well as a sensitizer are also suitable for efficient electron transfer with small reorganization energies.[9,10] In addition, rich and extensive absorption features of porphyrinoid systems guarantee increased absorption cross-sections and an efficient use of the solar spectrum.[9−11] Thus, a combination of both chromophores (i.e., porphyrins and fullerenes) seems ideal for fulfilling an enhanced light-harvesting efficiency of chromophores throughout the solar spectrum and a highly efficient conversion of the harvested light into the high energy state of the charge separation by photoinduced electron transfer.[12] Self-assembled monolayers (SAMs) have been made of fullerenes or porphyrins, and both have thereby merited special attention as artificial photosynthetic materials and photonic molecular devices.[13−20] However, such assemblies possess poor light-harvesting capability and also exhibit low values of the incident photon-to-photocurrent efficiency (IPCE).

We have previously reported a novel approach of enhancing the light-harvesting efficiency by electrodepositing $C_{60}$ films, from a cluster (aggregate) solution of acetonitrile/toluene (3:1, v/v), which absorb visible light strongly and exhibit much improved photoelectrochemical activity.[21] Although efforts have been made to employ donor−acceptor assembly (e.g., molecular dyads) in light energy harvesting applications, no such effort has been made to employ them in the form of clusters. Composites of donor and acceptor moieties (e.g., porphyrin and fullerene) in the form of clusters have yet to be assembled as a three-dimensional network on a conducting surface for attaining efficient photocurrent generation.[22] We report herein a simple and new approach of preparing composite clusters of porphyrin and fullerene in a mixture of polar and nonpolar solvents and assembling them on a nanostructured $SnO_2$ electrode using an electrophoretic deposition technique. Ways to improve photoelectrochemical behavior of the composite films of porphyrin−

* To whom correspondence should be addressed. E-mail: imahori@scl.kyoto.ac.jp; fukuzumi@ap.chem.eng.osaka-u.ac.jp; pkamat@nd.edu.
† University of Notre Dame.
‡ Osaka University.
§ Graduate School of Engineering, Kyoto University, PRESTO, Japan Science and Technology Agency.
|| Fukui Institute for Fundamental Chemistry, Kyoto University.

10.1021/jp035854v CCC: $25.00 
Published on Web 10/10/2003

fullerene clusters as compared to the single component films of porphyrin or fullerene clusters are discussed here.

## Experimental Section

**Materials and Methods.** Preparation of 5,15-bis(3,5-di-*tert*-butylphenyl)porphyrin) ($H_2P$) is described elsewhere.[23] Nanostructured $SnO_2$ films were cast on an optically transparent electrodes (OTEs) by applying a 2% colloidal solution obtained from Alfa Chemicals. The air-dried films were annealed at 673 K. Details on preparation of $SnO_2$ films on conducting glass substrates are reported elsewhere.[24] The $SnO_2$ film electrode is referred as OTE/$SnO_2$.

**Electrophoretic Deposition of Cluster Films.** A known amount (~2 mL) of $H_2P$, $C_{60}$, or mixed cluster solution in acetonitrile/toluene (3:1, v/v) was transferred to a 1-cm cuvette in which two electrodes (viz., OTE/$SnO_2$ and OTE) were kept at a distance of ~6 mm using a Teflon spacer. A dc voltage (500 V) was applied between these two electrodes using a Fluke 415 power supply. The deposition of the film can be seen as the solution becomes colorless with simultaneous brown coloration of the $SnO_2$/OTE electrode. The $SnO_2$/OTE electrode coated with mixed $H_2P$ and $C_{60}$ clusters is referred to as OTE/$SnO_2$/$(H_2P + C_{60})_n$.

The UV−visible spectra were recorded on a Shimadzu 3101 or a Cary 50 spectrophotometer. Transmission electron micrographs (TEM) of $C_{60}$ clusters were recorded by applying a drop of the sample to a carbon-coated copper grid. Images were recorded using a Hitachi H600 transmission electron microscope. AFM measurements were carried out using a Digital Nanoscope III in the tapping mode.

**Photoelectrochemical Measurements.** Photoelectrochemical measurements were carried out in a standard three-compartment cell consisting of a working electrode, a Pt wire gauze counter electrode, and a saturated calomel reference electrode (SCE). This configuration allows us to carry out photocurrent measurements under electrochemical bias. A Princeton Applied Research (PAR) model 173 potentiostat and a model 175 universal programmer were used for recording I−V characteristics. All other photoelectrochemical measurements were carried out using Pt gauge counter electrode in the same cell assembly using a Keithley model 617 programmable electrometer. The electrolyte was 0.5 M NaI and 0.01 M $I_2$ in acetonitrile. A collimated light beam from a 150-W xenon lamp with a 370 nm cutoff filter was used for excitation of $(H_2P + C_{60})_n$ films cast on $SnO_2$ electrodes. A Bausch and Lomb high-intensity grating monochromator was introduced into the path of the excitation beam for the selected wavelength.

## Results and Discussion

**Assembly of Free Base Porphyrin and $C_{60}$ as Molecular Clusters in Mixed Solvents.** $H_2P$ and $C_{60}$ are soluble in nonpolar solvents such as toluene, but sparingly soluble in polar solvents such as acetonitrile. When a concentrated solution of $C_{60}$ or $H_2P$ in toluene is mixed with acetonitrile by fast injection method, the molecules aggregate and form stable clusters.[21] The final solvent ratio of mixed solvent employed in the present experiments was 3:1 (v/v) acetonitrile/toluene. The same strategy can be extended to prepare mixed or composite molecular clusters consisting of $H_2P$ and $C_{60}$ molecules. Mixed cluster aggregates in the present investigation were prepared by mixing an equimolar solution of $H_2P$ and $C_{60}$ in toluene (0.5 mL) and then injecting it into a pool of acetonitrile (1.5 mL). These optically transparent composite clusters are stable at room temperature and they can be reverted back to their monomeric forms by diluting the solution with toluene.[21]

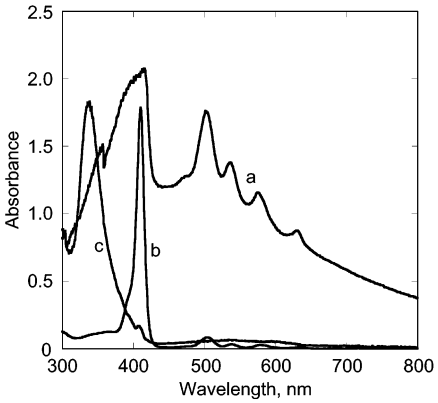


**Figure 1.** Absorption spectra of (a) $(H_2P + C_{60})_n$ in acetonitrile/toluene (3:1, v/v); $[H_2P] = [C_{60}] = 0.19$ mM, (b) 18 $\mu$M $H_2P$, and (c) 150 $\mu$M $C_{60}$ in toluene.

The absorption spectra of $H_2P$ and $C_{60}$ in neat toluene are compared with the absorption spectrum of $(H_2P + C_{60})_n$ clusters in acetonitrile/toluene (3:1, v/v) in Figure 1. The composite clusters $(H_2P + C_{60})_n$ in the mixed solvent (spectrum a) exhibit much broader and more intense absorption in the visible and near-infrared regions than those of parent $H_2P$ (spectrum b) and $C_{60}$ (spectrum c). Furthermore, the absorbance of $(H_2P + C_{60})_n$ in the visible and near-infrared regions increases with increasing concentrations of ($H_2P$ and $C_{60}$) (see Supporting Information Figure S1). Earlier studies on the porphyrin clusters have shown that the intermolecular interactions have significant impact on the intensity and position of the Soret and Q-bands.[25,26] The mixed clusters of $H_2P$ and $C_{60}$ prepared in acetonitrile and toluene show broader absorption bands corresponding to Soret and Q-bands of porphyrin. However, the presence of $C_{60}$ induces further enhancement of absorption of these clusters in the visible region. This demonstrates that the composite clusters of $H_2P$ and $C_{60}$ are superior light absorbers as compared to that of the single component clusters of $H_2P$ or $C_{60}$ because they absorb throughout the visible part of the solar spectrum. A charge-transfer type interaction between the two molecules may be responsible for the long-wavelength absorption of the composite clusters in Figure 1. Similar charge-transfer interactions leading to extended absorption have been observed for porphyrin−$C_{60}$ dyads linked at close proximity.[27,28]

Figure 2 shows transmission electron micrographs (TEM) images of the composite clusters, $(H_2P + C_{60})_n$. As the solvents evaporate on the copper grid the clusters form microcrystallites of well-defined shapes. TEM images of clusters of each component were also measured for comparison as shown in Supporting Information Figure S2. $H_2P$ clusters deposited on carbon grid have large particle sizes (~1 $\mu$m) and various shapes, whereas $C_{60}$ clusters form network structures with small particles (100−200 nm) (Figure S2). Totally different shapes of microcrystallites can be seen in the case of mixed cluster systems (Figure 2). The cluster size and shape for $(H_2P + C_{60})_n$ mixed clusters are dependent on the initial concentration of $H_2P$ and $C_{60}$ employed for preparing clusters. The clusters produced at relatively low concentrations (viz., $[H_2P] = [C_{60}] = 0.06$ mM) have fractal shaped tubules of ~500 nm length (Figure 2A), whereas those produced at a higher concentration ($[H_2P] = [C_{60}] = 0.25$ mM) have a square shape with a larger size of ~4 $\mu$m length (Figure 2B). It is interesting to note that the pattern observed throughout the grid indicates fairly uniform distribution of these crystallites while retaining the size and shape of individual crystallites.

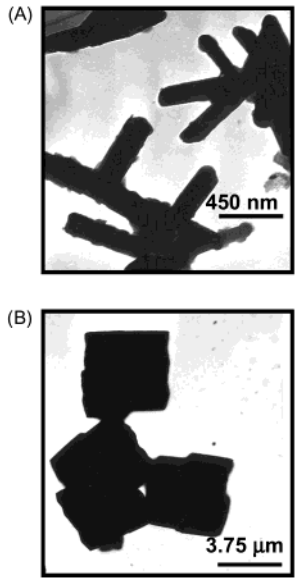


**Figure 2.** Transmission electron micrographs of clusters prepared with (A) $[H_2P] = [C_{60}] = 0.06$ mM and (B) $[H_2P] = [C_{60}] = 0.25$ mM in acetonitrile/toluene (3:1, v/v).

These electron micrographs indicate that the stacking of $H_2P$ clusters is influenced by the amount of $C_{60}$ concentration during the clustering effects. The interaction between the two molecules in the aggregated clusters plays an important role in dictating the growth of the microcrystallites. Recent studies have shown that porphyrins and fullerenes form supramolecular complexes, of which the majority contain closest contacts between one of the electron-rich 6:6 bonds of the guest fullerene and the geometric center of the host porphyrin.[29−33] The porphyrin−fullerene interaction energies are reported to be in the range from −16 to −18 kcal $mol^{-1}$.[34] Such a strong interaction between porphyrins and fullerenes is likely to be a good driving force for the formation of 1:1 composite clusters of $H_2P$ and $C_{60}$.

**Electrophoretic Deposition of Porphyrin−$C_{60}$ Mixed Clusters.** As shown earlier,[21] clusters of $C_{60}$ prepared in acetonitrile/toluene mixed solvent can be assembled electrophoretically as thin films on a conducting glass electrode surface. A similar electrodeposition approach was adopted to prepare film of $(H_2P + C_{60})_n$ on nanostructured $SnO_2$ films cast on an optically conducting glass electrode (referred as OTE/$SnO_2$). Upon application of the dc electric field of 500 V between OTE/$SnO_2$ and OTE electrodes, which were immersed parallel in a mixed acetonitrile/toluene (3:1, v/v) solution containing $(H_2P + C_{60})_n$ clusters, we can achieve deposition of mixed clusters on $SnO_2$ nanocrystallites. As the deposition continues we can visually observe discoloration of the solution and coloration of the electrode that is connected to the positive terminal of the dc power supply.

Figure 3 shows the absorption spectra of OTE/$SnO_2$/$(H_2P + C_{60})_n$ electrodes prepared using different precursor concentrations of $H_2P$ and $C_{60}$ in acetonitrile/toluene (3:1, v/v) mixture. Note that the mixed clusters were first prepared using different amounts of $H_2P$ and $C_{60}$ while maintaining their molar ratio 1:1. With increasing concentration we achieved higher cluster concentration in the solvent mixture and as a result of this we could achieve an increased amount of $H_2P$ and $C_{60}$ mixed cluster deposition on the $SnO_2$ film. An increase in the absorbance of OTE/$SnO_2$/$(H_2P + C_{60})_n$ in the visible and near-infrared regions with increasing concentration of $H_2P$ and $C_{60}$ is evident from Figure 3. We also found that at concentrations below 0.06 mM, the deposition of the composite clusters on the electrode as

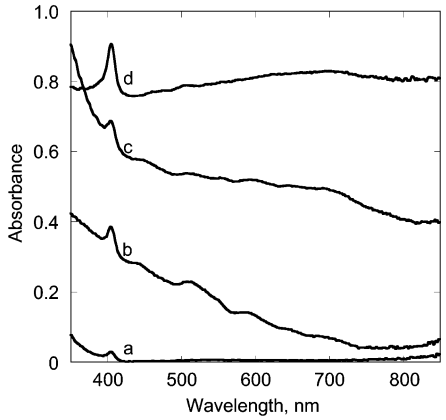


**Figure 3.** Absorption spectra of electrophoretically deposited $(H_2P + C_{60})_n$ films at an applied voltage of 500 V dc. The mixed cluster suspension consisted of equimolar concentrations of $H_2P$ and $C_{60}$ [(a) 0.06 mM, (b) 0.13 mM, (c) 0.19 mM, and (d) 0.25 mM].

**SCHEME 1: Formation and Growth of Composite Nanoclusters**

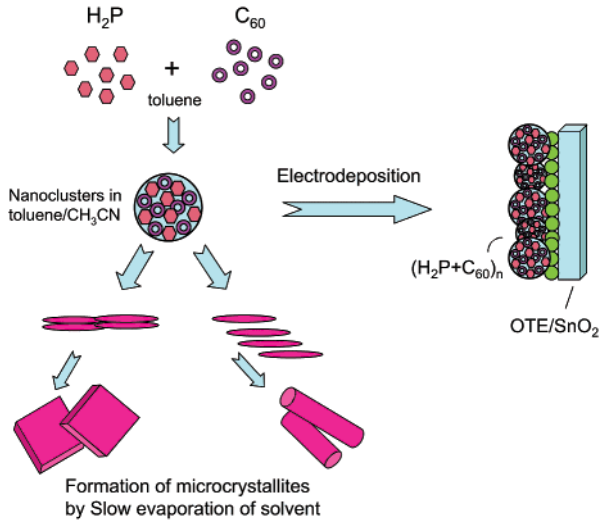


shown in Figure 3a produced relatively little absorbance changes. Hence, we employed concentrations of $H_2P$ and $C_{60}$ higher than 0.13 mM to obtain highly colored electrodes of $(H_2P + C_{60})_n$ clusters.

AFM was used to evaluate the topography of an OTE/$SnO_2$/$(H_2P + C_{60})_n$ film as shown in Figure 4. The OTE/$SnO_2$/$(H_2P + C_{60})_n$ film is composed of closely packed clusters of 200−300-nm size. It is interesting to note that the cluster size in the AFM image is much smaller than that observed in the TEM image of the composite clusters in acetonitrile/toluene (3:1, v/v) in Figure 2B. The formation of composite nanoclusters in mixed solvents and their growth as microcrystallites are illustrated in Scheme 1.

It is evident that electrophoretic deposition provides a quick deposition of nanosize mixed clusters under the influence of a dc electric field. Because of the quick rate of deposition the clusters fail to grow in the form of microcrystallites. Only the slow solvent evaporation technique employed during the preparation of the TEM grid allows the composite clusters to grow as well-defined microcrystallites. To attain high surface area for photosensitive electrodes, it is important to retain the molecular clusters in the nanosized regime. The AFM images show our success in attaining this goal.

**Photoelectrochemical Properties of OTE/$SnO_2$/$(H_2P + C_{60})_n$.** To further evaluate the photoelectrochemical performance

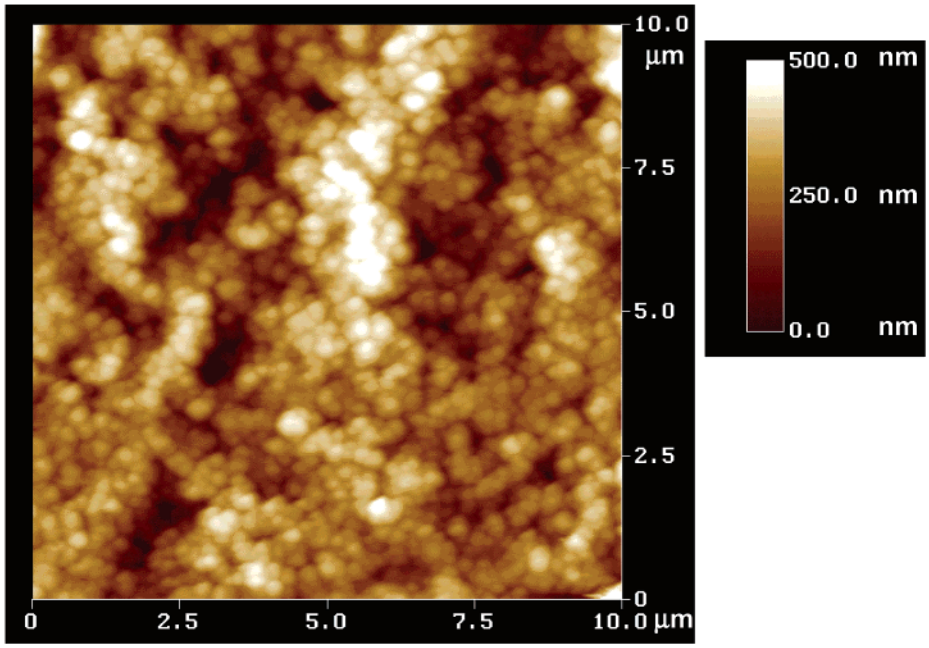


**Figure 4.** AFM image of the $(H_2P + C_{60})_n$ cluster film on an OTE/$SnO_2$ electrode ($[H_2P] = [C_{60}] = 0.25$ mM).

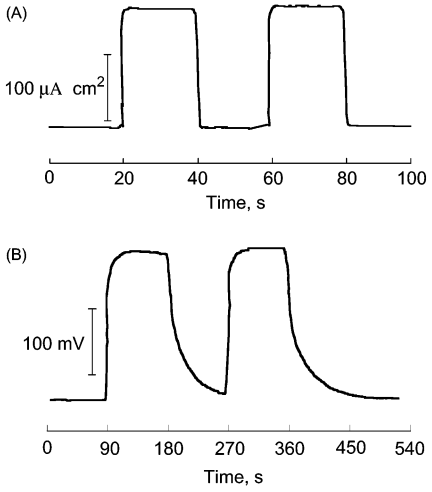


**Figure 5.** (A) Photocurrent response and (B) photovoltage response of OTE/$SnO_2$/$(H_2P+C_{60})_n$ electrode prepared from cluster solution of ($[H_2P] = [C_{60}] = 0.13$ mM) to visible light illumination ($\lambda > 370$ nm); electrolyte 0.5 M NaI and 0.01 M $I_2$ in acetonitrile; input power 110 mW/cm$^2$.

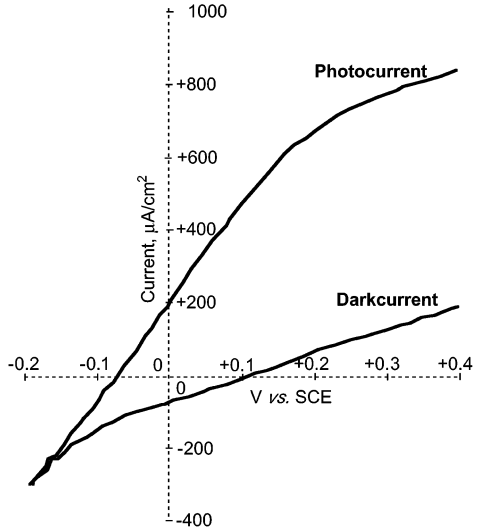


**Figure 6.** I−V characteristics of OTE/$SnO_2$/$(H_2P+C_{60})_n$ electrode prepared from cluster solution of ($[H_2P] = [C_{60}] = 0.19$ mM) under white light ($\lambda > 370$ nm) illumination; electrolyte 0.5 M NaI and 0.01 M $I_2$ in acetonitrile; input power 110 mW/cm$^2$.

of the $(H_2P + C_{60})_n$ films we used an OTE/$SnO_2$/$(H_2P + C_{60})_n$ electrode as a photoanode in a photoelectrochemical cell. Photocurrent measurements were performed in acetonitrile containing NaI (0.5 M) and $I_2$ (0.01 M) as redox electrolyte and Pt gauge counter electrode. The photocurrent and photovoltage responses recorded following the excitation of OTE/$SnO_2$/$(H_2P + C_{60})_n$ electrode in the visible light region ($\lambda >$ 370 nm) are shown in Figure 5A and B, respectively. The photocurrent response is prompt, steady, and reproducible during repeated on/off cycles of the visible light illumination. The short circuit photocurrent density ($i_{sc}$) of 180 $\mu$A/cm$^2$ and open circuit voltage ($V_{oc}$) of 210 mV were reproducibly obtained during these measurements. Blank experiments conducted with OTE/$SnO_2$ (i.e., by excluding composite clusters $(H_2P + C_{60})_n$) produced no detectable photocurrent under similar experimental conditions. These experiments confirmed the role of $(H_2P + C_{60})_n$ assembly toward harvesting light energy and generating photocurrent during the operation of a photoelectrochemical cell.

The charge separation in the OTE/$SnO_2$/$(H_2P + C_{60})_n$ electrode assembly can be further modulated by the application of an electrochemical bias. Figure 6 shows I−V characteristics of the OTE/$SnO_2$/$(H_2P + C_{60})_n$ electrode under the visible light illumination. The photocurrent increases as the applied potential is scanned toward more positive potentials. Increased charge separation and the facile transport of charge carriers under positive bias are responsible for enhanced photocurrent generation. At potentials greater than +0.4 V vs SCE direct electrochemical oxidation of iodide interferes with the photocurrent measurement.

We also evaluated the power characteristics of the photoelectrochemical cell by varying the load resistance. A drop in the photovoltage and an increase in the photocurrent are observed with decreasing the load resistance (Figure 7). The fill factor ($ff = P_{max}/(V_{oc} \times i_{sc})$), where $P_{max}$ is the maximum power output of the cell, $V_{oc}$ is open circuit photovoltage, and $i_{sc}$ is the short circuit photocurrent) for the $(H_2P + C_{60})_n$-based

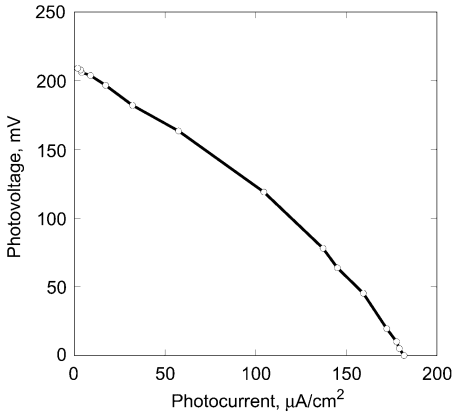


**Figure 7.** Power characteristics of the photoelectrochemical cell under white light ($\lambda > 370$ nm) illumination. Electrode: OTE/$SnO_2$/($H_2P$ + $C_{60}$)$_n$ electrode prepared from cluster solution of ([$H_2P$] = [$C_{60}$] = 0.13 mM) and Pt counter electrode; electrolyte 0.5 M NaI and 0.01 M $I_2$ in acetonitrile; input power 110 mW/cm$^2$.

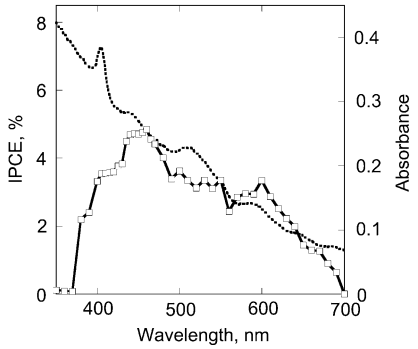


**Figure 8.** The photocurrent action spectrum (presented in terms of % IPCE) of OTE/$SnO_2$/($H_2P$ + $C_{60}$)$_n$ electrode prepared from cluster solution of ([$H_2P$] = [$C_{60}$] = 0.13 mM) (solid line). Dashed line shows the absorption spectrum of the electrode.

photoelectrochemical cell was determined to be 0.35. The low fill factor observed in the present experiment shows the need to overcome the factors limiting charge transport and redox processes. Net power conversion efficiency obtained for the same cell was 0.012% (input power 110 mW/cm$^2$). At low intensity excitation (3.4 mW/cm$^2$), the efficiency is increased up to 0.037%. Both the I−V characteristics and the intensity dependence of the efficiency show that charge recombination and charge transport within the nanostructure assembly are major limiting factors in achieving higher photoconversion efficiencies.

To evaluate the response of ($H_2P$ + $C_{60}$)$_n$ clusters toward the photocurrent generation a series of photocurrent action spectra were recorded and compared against the absorption spectra. The photocurrent action spectrum of OTE/$SnO_2$/($H_2P$ + $C_{60}$)$_n$ produced by the electrodeposition of $H_2P$ and $C_{60}$ ([$H_2P$] = [$C_{60}$] = 0.13 mM) is shown in Figure 8 (solid line) together with the absorption spectrum of the electrode (dashed line).[35] The IPCE values were calculated by normalizing the photocurrent values for incident light energy and intensity and using the expression 1[36]

$$\text{IPCE (\%)} = 100 \times 1240 \times i_{sc}/(I_{inc} \times \lambda) \qquad (1)$$

where $i_{sc}$ is the short circuit photocurrent (A/cm$^2$), $I_{inc}$ is the incident light intensity (W/cm$^2$), and $\lambda$ is the wavelength (nm). The overall response of the OTE/$SnO_2$/($H_2P$ + $C_{60}$)$_n$ parallels the broad absorption spectral features indicating the involvement of $H_2P$ and $C_{60}$ in the photocurrent generation.[37]

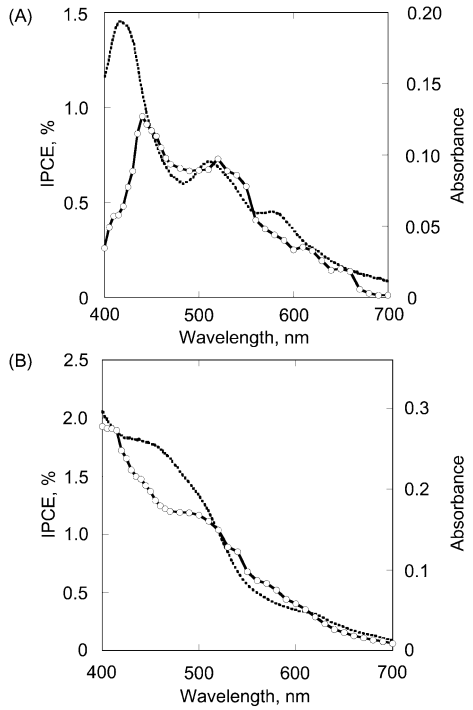


**Figure 9.** Photocurrent action spectra (presented in terms of % IPCE) of (A) OTE/$SnO_2$/($H_2P$)$_n$ electrode prepared from cluster solution of ([$H_2P$] = 0.13 mM) (solid line) and (B) OTE/$SnO_2$/($C_{60}$)$_n$ electrode prepared from cluster solution of ([$C_{60}$] = 0.13 mM) (solid line). Dashed line shows the absorption spectra of the corresponding electrode.

**TABLE 1: Comparison of Incident Photon Conversion and Light Harvesting Efficiencies for the $H_2P$ and $C_{60}$ Cluster Systems; IPCE and LHE Values of OTE/$SnO_2$/($H_2P$ + $C_{60}$)$_n$, OTE/$SnO_2$/($C_{60}$)$_n$, and OTE/$SnO_2$/($C_{60}$)$_n$ at 430 nm**

| $H_2P$ (mM)[a] | $C_{60}$ (mM)[a] | IPCE at 430 nm (%)[b] | LHE at 430 nm (%)[c] |
|---|---|---|---|
| 0.13 | 0 | 0.6 | 2.2 |
| 0 | 0.13 | 1.6 | 3.9 |
| 0.13 | 0.13 | 4.5 | 10 |

[a] Final concentration of OTE/$SnO_2$/($H_2P$ + $C_{60}$)$_n$ electrode. [b] IPCE values at 430 nm. [c] Light harvesting efficiency (LHE) values at 430 nm, LHE (%) = IPCE (%)/$F_A$ ($F_A$ is the fraction of the absorbed light as determined from the absorbance of the film at 430 nm).

We also compared the individual contributions from $H_2P$ and $C_{60}$ clusters by preparing these clusters separately in acetonitrile/toluene (3:1, v/v) and then depositing them on OTE/$SnO_2$ electrodes using an electrophoretic approach. The photoelectrochemical measurements of OTE/$SnO_2$/($H_2P$)$_n$ and OTE/$SnO_2$/($C_{60}$)$_n$ were performed under the same experimental conditions as those employed in Figure 8. The photocurrent action spectra of OTE/$SnO_2$/($H_2P$)$_n$ and OTE/$SnO_2$/($C_{60}$)$_n$ are shown in Figure 9A and B (solid lines) together with the absorption spectra of the electrodes (dashed lines), respectively. The photocurrent action spectra of OTE/$SnO_2$/($H_2P$)$_n$ and OTE/$SnO_2$/($C_{60}$)$_n$ match with the absorption spectra of the electrode (Figure 9A and B). Such an agreement between photocurrent action spectra and the absorption spectra indicates that the excited states of porphyrin and fullerene are capable of generating photocurrent. Note that the maximum IPCE values observed in these two individual systems [0.6% for OTE/$SnO_2$/($H_2P$)$_n$ and 1.6% for OTE/$SnO_2$/($C_{60}$)$_n$, respectively, at 430 nm] are lower than that observed in mixed cluster systems (IPCE = 4.0%).

We also compared the light harversting efficiency (LHE) or internal quantum efficienty of these two electrodes by accounting for the fraction of the absorbed light. Table 1 summarizes

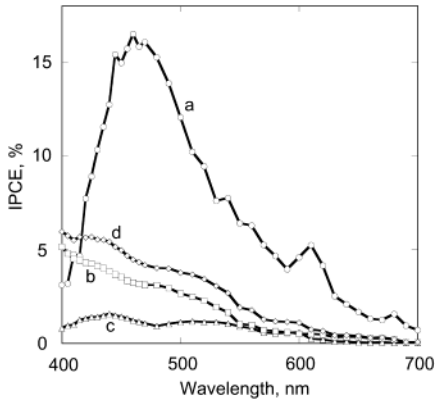


**Figure 10.** Comparison of photocurrent response (IPCE values) of (a) OTE/$SnO_2$/($H_2P$ + $C_{60}$)$_n$ electrode prepared from cluster solution of ([$H_2P$] = [$C_{60}$] = 0.19 mM), (b) OTE/$SnO_2$/($C_{60}$)$_n$ electrode prepared from cluster solution of ([$C_{60}$] = 0.19 mM), (c) OTE/$SnO_2$/($H_2P$)$_n$ electrode prepared from cluster solution of ([$H_2P$] = 0.19 mM), and (d) the sum of the IPCE response of OTE/$SnO_2$/($C_{60}$)$_n$ (b) and OTE/$SnO_2$/($H_2P$)$_n$ (c); an applied bias potential 0.2 V vs SCE, electrolyte 0.5 M NaI, and 0.01 M $I_2$ in acetonitrile.

the IPCE and LHE values for two sets of experiments performed using 0.13 mM of $H_2P$ and $C_{60}$ in the mixed clusters. The LHE for the lower concentration followed the same trend as that of IPCE with a maximum efficiency of 10% under unbiased conditions. This result implies that absorbed photon is more effectively converted into photocurrent in a mixed clusters system than in the individual systems. The obvious question is what mechanism dictates the cooperative effect between the $H_2P$ and $C_{60}$ during photoexcitation of composite clusters.

**Mechanism of Photocurrent Generation.** We further compared the photocurrent action spectra of OTE/$SnO_2$/($H_2P$ + $C_{60}$)$_n$ with those of OTE/$SnO_2$/($C_{60}$)$_n$ and OTE/$SnO_2$/($H_2P$)$_n$ by using them in a standard three-compartment cell as a working electrode along with a Pt wire gauze counter electrode and saturated calomel reference electrode (SCE) (Figure 10). The photocurrent action spectrum of OTE/$SnO_2$/($H_2P$ + $C_{60}$)$_n$ prepared by the electrodeposition of mixed clusters (prepared from 0.19 mM of $H_2P$ and 0.19 mM $C_{60}$ solutions) shows a maximum IPCE value of 17% at an applied potential of 0.2 V vs SCE (spectrum a in Figure 10). Under the same experimental conditions we observed much smaller IPCE values for the single component systems, viz., OTE/$SnO_2$/($C_{60}$)$_n$ and OTE/$SnO_2$/($H_2P$)$_n$ (spectra b and c in Figure 10). If the observed effect was an additive effect arising from the two components we would have expected to see the spectrum as represented by spectrum d in Figure 10. Surprisingly, the sum of the two individual IPCE values (~6%) of the individual systems is much smaller than the IPCE value obtained with the mixed cluster system (17%), viz. OTE/$SnO_2$/($H_2P$ + $C_{60}$)$_n$. Such an enhancement in the photocurrent generation of the composite cluster systems of $H_2P$ and $C_{60}$ indicates an interplay between excited porphyrin and $C_{60}$ may be a dominating factor. This is in contrast to individual systems in which the excited sensitizer undergoes either reduction by iodide ion or charge injection into semiconductor nanocrystallites. In the case of OTE/$SnO_2$/($C_{60}$)$_n$, photoinduced electron transfer between iodide ion and the excited state of $C_{60}$ clusters is the primary step in the photocurrent generation.[21] The reduced $C_{60}$ then injects electrons into $SnO_2$ nanocrystallites. This mechanism of photochemically generating electroactive species ($C_{60}$ anion in the present example) illustrated is commonly operative in photogalvanic type solar cells (Scheme 2).

**SCHEME 2: Photoinduced Electron Transfer at an OTE/$SnO_2$/($C_{60}$)$_n$ Electrode**

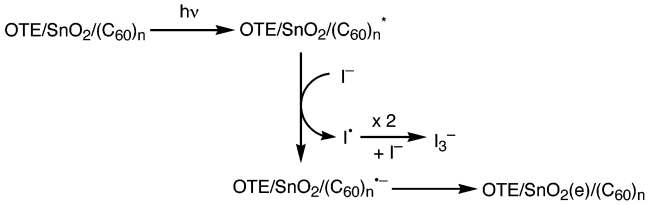


**SCHEME 3: Photoinduced Charge Transfer at an OTE/$SnO_2$/($H_2P$)$_n$ Electrode**

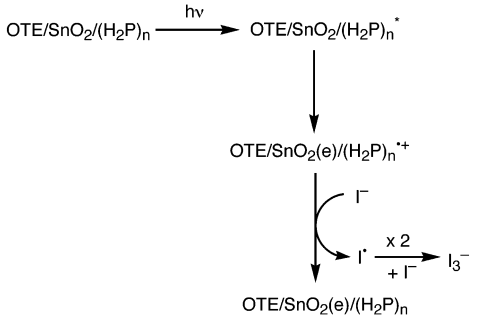


**SCHEME 4: Photoinduced Charge Transfer at an OTE/$SnO_2$/($H_2P$ + $C_{60}$)$_n$ Electrode**

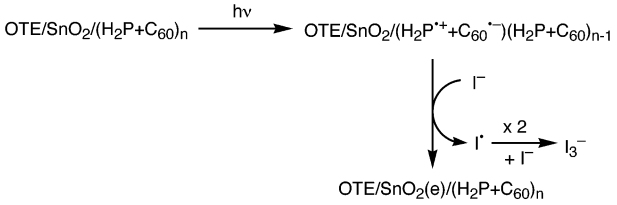


On the other hand, in OTE/$SnO_2$/($H_2P$)$_n$ system, the excited state of $H_2P$ being a good electron donor injects an electron from the excited state of $H_2P$ clusters to $SnO_2$ nanocrystallites. Similar charge injection processes involving porphyrin derivatives have been studied earlier.[38] The charge injection mechanism leading to the photocurrent generation is illustrated in Scheme 3.

If Schemes 2 and 3 were the only two pathways dominating the photocurrent generation in the mixed cluster system, we would have expected to see an additive effect, i.e., the photocurrent response similar to spectrum d in Figure 10. However, we observe a significantly enhanced IPCE for the mixed cluster system. The major pathway contributing to the enhanced photocurrent generation in the composite system OTE/$SnO_2$/($H_2P$ + $C_{60}$)$_n$ is the intermolecular charge transfer between excited $H_2P$ and $C_{60}$ within the cluster to produce $H_2P^{\bullet+}$ and $C_{60}^{\bullet-}$. Photoinduced electron transfer from the porphyrin singlet excited state ($^1H_2P^*$) to $C_{60}$ is thermodynamically feasible as evident from the oxidation potential of $^1H_2P^*$ ($^1H_2P^*/H_2P^{\bullet+}$ = −0.7 V vs NHE)[7c] which is more negative than the reduction potential of $C_{60}$ ($C_{60}/C_{60}^{\bullet-}$ = −0.2 V vs NHE).[21] Photoinduced electron transfer between the excited porphyrin and $C_{60}$ has been investigated in detail in earlier studies.[7,11,39] Additionally, $C_{60}^{\bullet-}$ is also generated from the interaction between excited $C_{60}$ ($C_{60}^*$) and iodide ions present in the electrolyte. Collectively, these $C_{60}^{\bullet-}$ species accumulated in clusters transfer electrons to $SnO_2$ nanocrystallites ($E_{CB}$ = 0 V vs NHE),[21,36] to produce the current in the circuit. These reaction steps leading to the photocurrent generation are illustrated in Scheme 4. The regeneration of $H_2P$ clusters ($H_2P/H_2P^{\bullet+}$ = 1.2 V vs NHE)[7c] is achieved by the

triiodide/iodide couple ($I_3^-/I^- = 0.5$ V vs NHE)[21,36] present in the electrolyte system.

The results described in this study highlight a simple and convenient way to design donor−acceptor type molecular clusters that can be tailored to harvest light energy efficiently. Careful screening of donor and acceptor moieties in molecular clusters is currently underway to further improve the photoconversion efficiencies.

## Conclusion

Broader absorption in the visible and near-infrared region and enhanced photocurrent generation efficiencies of composite molecular nanoclusters show their usefulness in light harvesting applications. By employing an electrodeposition method to construct the composite cluster electrodes [OTE/$SnO_2$/($H_2P$ + $C_{60}$)$_n$] we have demonstrated remarkable photoelectrochemical activity of a donor−acceptor cluster system in the visible region. The incident phototo-photocurrent efficiency (IPCE) of 17% obtained for the mixed cluster system is significantly higher than the sum of the IPCE values obtained with individual cluster systems, viz., OTE/$SnO_2$/($C_{60}$)$_n$ and OTE/$SnO_2$/($H_2P$)$_n$.

**Acknowledgment.** This work was partially supported by a Grant-in-Aid from the Ministry of Education, Culture, Sports, Science and Technology, Japan. T.H. thanks a 21st Century COE program of Osaka University for financial support during his stay at Notre Dame Radiation laboratory. P.V.K. acknowledges support from the Office of Basic Energy Science of the U. S. Department of the Energy. This is contribution NDRL 4464 from the Notre Dame Radiation Laboratory and from Osaka University.

**Supporting Information Available:** Absorption spectra of ($H_2P$ + $C_{60}$)$_n$ in acetonitrile/toluene (3:1, v/v) at different concentrations of $H_2P$ and $C_{60}$ (Figure S1); transmission electron micrographs of ($H_2P$)$_n$ and ($C_{60}$)$_n$ (Figure S2); and the photocurrent action spectra of OTE/$SnO_2$/($H_2P$ + $C_{60}$)$_n$ prepared from different concentrations of $H_2P$ and $C_{60}$ (Figure S3). This material is available free of charge via the Internet at http://pubs.acs.org.

## References and Notes

(1) (a) Hagfeldt, A.; Grätzel, M. *Chem. Rev.* **1995**, *95*, 49. (b) Bonhôte, P.; Moser, J.-E.; Humphry-Baker, R.; Vlachopoulos, N.; Zakeeruddin, S. M.; Walder, L.; Grätzel, M. *J. Am. Chem. Soc.* **1999**, *121*, 1324. (c) Hagfeldt, A.; Grätzel, M. *Acc. Chem. Res.* **2000**, *33*, 269.

(2) (a) O'Regan, B.; Grätzel, M. *Nature* **1991**, *353*, 737. (b) Bach, U.; Lupo, D.; Comte, P.; Moser, J. E.; Weissörtel, F.; Salbeck, J.; Spreitzer, H.; Grätzel, M. *Nature* **1998**, *395*, 583.

(3) Cinnsealach, R.; Boschloo, G.; Rao, S. N.; Fitzmaurice, D. *Sol. Energy Mater. Sol. Cells* **1999**, *55*, 215.

(4) Shah, A.; Torres, P.; Tscharner, R.; Wyrsch, N.; Keppner, H. *Science* **1999**, *285*, 692.

(5) (a) Granström, M.; Petrisch, K.; Arias, A. C.; Lux, A.; Andersson, M. R.; Friend, R. H. *Nature* **1998**, *395*, 257. (b) Halls, J. J. M.; Walsh, C. A.; Greenham, N. C.; Marseglia, E. A.; Friend, R. H.; Moratti, S. C.; Holmes, A. B. *Nature* **1995**, *376*, 498.

(6) Yu, G.; Gao, J.; Hummelen, J. C.; Wudl, F.; Heeger, A. J. *Science* **1995**, *270*, 1789.

(7) (a) Fukuzumi, S.; Imahori, H. In *Electron Transfer in Chemistry*; Balzani, V., Ed.; Wiley-VCH: Weinheim, 2001; Vol. 2, pp 927−975. (b) Imahori, H.; Sakata, Y. *Eur. J. Org. Chem.* **1999**, 2445. (c) Imahori, H.; Mori, Y.; Matano, Y. *J. Photochem. Photobiol. C* **2003**, *4*, 51.

(8) (a) Fukuzumi, S.; Guldi, D. M. In *Electron Transfer in Chemistry*; Balzani, V., Ed.; Wiley-VCH: Weinheim, 2001; Vol. 2, pp 270−337. (b) Fukuzumi, S.; Ohkubo, K.; Imahori, H.; Guldi, D. M. *Chem. Eur. J.* **2003**, *9*, 1585.

(9) Fukuzumi, S. In *The Porphyrin Handbook*; Kadish, K. M., Smith, K. M., Guilard, R., Eds.; Academic Press: San Diego, CA, 2000; Vol. 8, pp 115−152.

(10) Fukuzumi, S.; Endo, Y.; Imahori, H. *J. Am. Chem. Soc.* **2002**, *124*, 10974.

(11) Gust, D.; Moore, T. A. In *The Porphyrin Handbook*; Kadish, K. M., Smith, K. M., Guilard, R., Eds.; Academic Press: San Diego, CA, 2000; Vol. 8, pp 153−190.

(12) (a) Fukuzumi, S. *Pure Appl. Chem.* **2003**, *75*, 577. (b) Fukuzumi, S. *Org. Biomol. Chem.* **2003**, *1*, 609.

(13) (a) Shi, X.; Caldwell, W. B.; Chen, K.; Mirkin, C. A. *J. Am. Chem. Soc.* **1994**, *116*, 11598. (b) Caldwell, W. B.; Chen, K.; Mirkin, C. A.; Babinec, S. J. *Langmuir* **1993**, *9*, 1945. (c) Shon, Y.-S.; Kelly, K. F.; Halas, N. J.; Lee, T. R. *Langmuir* **1999**, *15*, 5329. (d) Hatano, T.; Ikeda, A.; Akiyama, T.; Yamada, S.; Sano, M.; Kanekiyo, Y.; Shinkai, S. *J. Chem. Soc., Perkin Trans. 2* **2000**, *5*, 909.

(14) (a) Arias, F.; Godínez, L. A.; Wilson, S. R.; Kaifer, A. E.; Echegoyen, L. *J. Am. Chem. Soc.* **1996**, *118*, 6086. (b) Echegoyen, L.; Echegoyen, L. E. *Acc. Chem. Res.* **1998**, *31*, 593. (c) Liu, S.-G.; Martineau, C.; Raimundo, J.-M.; Roncali, J.; Echegoyen, L. *Chem. Commun.* **2001**, 913.

(15) (a) Imahori, H.; Azuma, T.; Ajavakom, A.; Norieda, H.; Yamada, H.; Sakata, Y. *J. Phys. Chem. B* **1999**, *103*, 7233. (b) Hirayama, D.; Takimiya, K.; Aso, Y.; Otsubo, T.; Hasobe, T.; Yamada, H.; Imahori, H.; Fukuzumi, S.; Sakata, Y. *J. Am. Chem. Soc.* **2002**, *124*, 532.

(16) (a) Lahav, M.; Gabriel, T.; Shipway, A. N.; Willner, I. *J. Am. Chem. Soc.* **1999**, *121*, 258. (b) Lahav, M.; Heleg-Shabtai, V.; Wasserman, J.; Katz, E.; Willner, I.; Dürr, H.; Hu, Y.-Z.; Bossmann, S. H. *J. Am. Chem. Soc.* **2000**, *122*, 11480. (c) Uosaki, K.; Kondo, T.; Zhang, X.-Q.; Yanagida, M. *J. Am. Chem. Soc.* **1997**, *119*, 8367. (d) Abdelrazzaq, F. B.; Kwong, R. C.; Thompson, M. E. *J. Am. Chem. Soc.* **2002**, *124*, 4796.

(17) (a) Katz, E.; Willner, I. *Langmuir* **1997**, *13*, 3364. (b) Zak, J.; Yuan, H.; Ho, M.; Woo, L. K.; Porter, M. D. *Langmuir* **1993**, *9*, 2772. (c) Hutchison, J. E.; Postlethwaite, T. A.; Chen, C.-h.; Hathcock, K. W.; Ingram, R. S.; Ou, W.; Linton, R. W.; Murray, R. W.; Tyvoll, T. A.; Chng, L. L.; Collman, J. P. *Langmuir* **1997**, *13*, 2143. (d) Hutchison, J. E.; Postlethwaite, T. A.; Murray, R. W. *Langmuir* **1993**, *9*, 3277. (e) Simpson, T. R. E.; Revell, D. J.; Cook, M. J.; Russell, D. A. *Langmuir* **1997**, *13*, 460. (f) Gryko, D. T.; Zhao, F.; Yasseri, A. A.; Roth, K. M.; Bocian, D. F.; Kuhr, W. G.; Lindsey, J. S. *J. Org. Chem.* **2000**, *65*, 7356.

(18) (a) Ashkenasy, G.; Kalyuzhny, G.; Libman, J.; Rubinstein, I.; Shanzer, A. *Angew. Chem., Int. Ed.* **1999**, *38*, 1257. (b) Kanayama, N.; Kanbara, T.; Kitano, H. *J. Phys. Chem. B* **2000**, *104*, 271. (c) Offord, D. A.; Sachs, S. B.; Ennis, M. S.; Eberspacher, T. A.; Griffin, J. H.; Chidsey, C. E. D.; Collman, J. P. *J. Am. Chem. Soc.* **1998**, *120*, 4478. (d) Willner, I.; Heleg-Shabtai, V.; Katz, E.; Rau, H. K.; Haehnel, W. *J. Am. Chem. Soc.* **1999**, *121*, 6455.

(19) (a) Imahori, H.; Norieda, H.; Ozawa, S.; Ushida, K.; Yamada, H.; Azuma, T.; Tamaki, K.; Sakata, Y. *Langmuir* **1998**, *14*, 5335. (b) Imahori, H.; Norieda, H.; Nishimura, Y.; Yamazaki, I.; Higuchi, K.; Kato, N.; Motohiro, T.; Yamada, H.; Tamaki, K.; Arimura, M.; Sakata, Y. *J. Phys. Chem. B* **2000**, *104*, 1253.

(20) (a) Imahori, H.; Norieda, H.; Yamada, H.; Nishimura, Y.; Yamazaki, I.; Sakata, Y.; Fukuzumi, S. *J. Am. Chem. Soc.* **2001**, *123*, 100. (b) Yamada, H.; Imahori, H.; Nishimura, Y.; Yamazaki, I.; Fukuzumi, S. *Adv. Mater.* **2002**, *14*, 892. (c) Imahori, H.; Fukuzumi, S. *Adv. Mater.* **2001**, *13*, 1197.

(21) (a) Kamat, P. V.; Barazzaiyuk, S.; Thomas, K. G.; Hotchandani, S. *J. Phys. Chem. B* **2000**, *104*, 4014. (b) Sudeep P. K.; Ipe, B. I.; Thomas, K. G.; George, M. V.; Barazzouk, S.; Hotchandai, S.; Kamat, P. V. *Nano. Lett.* **2002**, *2*, 29. (c) Kamat, P. V.; Barazzouk, S.; Hotchandani, S. Thomas, K. G. *Chem. Eur. J.* **2000**, *6*, 3914.

(22) A previous attempt to use clusters of a porphyrin−fullerene dyad linked by a covalent bond deposited on nanostructured $SnO_2$ films using an electrophoretic technique afforded only a small IPCE value (∼0.4%) under visible light excitation; see Imahori, H.; Hasobe, T.; Yamada, H.; Kamat, P. V.; Barazzouk, S.; Fujitsuka, M.; Ito, O.; Fukuzumi, S. *Chem. Lett.* **2001**, 784. A better result was reported for a porphyrin−fullerene dyad adsorbed on ITO/$SnO_2$; see Fungo, F.; Otero, L.; Borsarelli, C. D.; Durantini, E. N.; Silber, J. J.; Sereno, L. *J. Phys. Chem. B* **2002**, *106*, 4070.

(23) Imahori, H.; Tamaki, K.; Araki, Y.; Sekiguchi, Y.; Ito, O.; Sakata Y.; Fukuzumi, S. *J. Am. Chem. Soc.* **2002**, *124*, 5165.

(24) Bedja, I.; Hotchandani, S.; Kamat, P. V. *J. Phys. Chem.* **1994**, *98*, 4133.

(25) Siggel, U.; Bindig, U.; Endish, C.; Komatsu, T.; Tsuchida, E.; Voigt, J.; Fuhrhop, J.-H. *Ber. Bunsen-Ges. Phys. Chem.* **1996**, *12*, 2070.

(26) (a) Kim, Y.-S.; Liang, K.; Law, K.-Y.; Whitten, D. G.; *J. Phys. Chem.* **1994**, *98*, 984. (b) Wu, D.-G.; Huang, C.-H.; Gan, L.-B.; Zhang, W.; Zheng, J. *J. Phys. Chem. B* **1999**, *103*, 4377. (c) Wu, D.-G.; Huang, Y.-Y.; Huang, C.-H.; Gan, L.-B. *J. Chem. Soc., Faraday Trans.* **1998**, *94*, 1411. (d) Nasr, C.; Liu, D.; Hotchandai, S.; Kamat, P. V. *J. Phys. Chem.* **1996**, *100*, 11054. (e) Xia, W. S.; Huang, C. H.; Luo, C. P.; Gan, L. B.; Chen, Z. D. *J. Phys. Chem.* **1996**, *100*, 15525. (f) Wu, D.-G.; Huang, C.-H.; Gan, L.-B.; Huang, Y.-Y. *Langmuir* **1998**, *14*, 3783.

(27) (a) D'Souza, F.; Gadde, S.; Zandler, M. E.; Arkady, K.; El-Khouly, M. E.; Fujitsuka, M.; Ito, O. *J. Phys. Chem. A* **2002**, *106*, 12393. (b) Guldi, D. M.; Luo, C.; Prato, M.; Troisi, A.; Zerbetto, F.; Scheloske, M.; Dietel, E.; Bauer, W.; Hirsch, A. *J. Am. Chem. Soc.* **2001**, *123*, 9166. (c) Schuster, D. I.; Jarowski, P. D.; Kirschner, A. N.; Wilson, S. R. *J. Mater. Chem.* **2002**, *12*, 2041. (d) Olmstead, M. M.; de Bettencourt-Dias, A.; Duchamp,

J. C.; Stevenson, S.; Marciu, D.; Dorn, H. C.; Balch, A. L. *Angew. Chem., Int. Ed.* **2001**, *40*, 1223.

(28) Tkachenko, N. V.; Rantala, L.; Tauber, A. Y.; Helaja, J.; Hynninen, P. H.; Lemmetyinen, H. *J. Am. Chem. Soc.* **1999**, *121*, 9378.

(29) Diederich, F.; Gómez-Löpez, M. *Chem. Soc. Rev.* **1999**, *28*, 263.

(30) (a) Boyd, P. D. W.; Hodgson, M. C.; Rickard, C. E. F.; Oliver, A. G.; Chaker, L.; Brothers, P. J.; Bolskar, R. D.; Tham, F. S.; Reed, C. A. *J. Am. Chem. Soc*. **1999**, *121*, 10487. (b) Sun, D.; Tham, F. S.; Reed, C. A.; Chaker, L.; Burgess, M.; Boyd, P. D. W. *J. Am. Chem. Soc.* **2000**, *122*, 10704. (c) Sun, D.; Tham, F. S.; Reed, C. A.; Chaker, L.; Boyd, P. D. W. *J. Am. Chem. Soc*. **2002**, *124*, 6604. (d) Sun, D.; Tham, F. S.; Reed, C. A.; Boyd, P. D. W. *Proc. Natl. Acad. Sci. U.S.A.* **2002**, *99*, 5088.

(31) (a) Olmstead, M. M.; Costa, D. A.; Maitra, K.; Noll, B. C.; Phillips, S. L.; Van Calcar, P. M.; Balch, A. L. *J. Am. Chem. Soc*. **1999**, *121*, 7090. (b) Olmstead, M. M.; de Bettencourt-Dias, A.; Duchamp, J. C.; Stevenson, S.; Marciu, D.; Dorn, H. C.; Balch, A. L. *Angew. Chem., Int. Ed*. **2001**, *40*, 1223.

(32) (a) Tashiro, K.; Aida, T.; Zheng, J.-Y.; Kinbara, K.; Saigo, K.; Sakamoto, S.; Yamaguchi, K. *J. Am. Chem. Soc*. **1999**, *121*, 9477. (b) Zheng, J.-Y.; Tashiro, K.; Hirabayashi, Y.; Kinbara, K.; Saigo, K.; Aida, T.; Sakamoto, S.; Yamaguchi, K. *Angew. Chem., Int. Ed.* **2001**, *40*, 1857.

(33) (a) Guldi, D. M.; Luo, C.; Prato, M.; Troisi, A.; Zerbetto, F.; Scheloske, M.; Dietel, E.; Bauer, W.; Hirsch, A. *J. Am. Chem. Soc.* **2001**, *123*, 9166. (b) Imahori, H.; Hagiwara, K.; Aoki, M.; Akiyama, T.; Taniguchi, S.; Okada, T.; Shirakawa, M.; Sakata, Y. *J. Am. Chem. Soc.* **1996**, *118*, 11771.

(34) Wang, Y.-B.; Lin, Z. *J. Am. Chem. Soc.* **2003**, *125*, 6072.

(35) For photocurrent action spectra of OTE/$SnO_2$/$(H_2P)_n$ prepared from different concentrations of $H_2P$ and $C_{60}$; see Supporting Information Figure S3.

(36) Khazraji, A. C.; Hotchandani, S.; Das, S.; Kamat P. V. *J. Phys. Chem. B* **1999**, *103*, 4693.

(37) The IPCE value drops to zero in the longer wavelength region ($\lambda > 700$ nm), where the electrode still has significant light absorption. The broad absorption band in the long-wavelength region is ascribed to the charge transfer (CT) band of the intermolecular $H_2P-C_{60}$ $\pi$-complex of the clusters (vide supra). The direct photoexcitation of the CT band results in formation of the exciplex, which generally has a short lifetime, leading to no photocurrent generation. See Imahori, H.; Tkachenko, N. V.; Vehmanen, V.; Tamaki, K.; Lemmetyinen, H.; Sakata, Y.; Fukuzumi, S. *J. Phys. Chem. A* **2001**, *105*, 1750.

(38) (a) Pileni, M. P.; Grätzel, M. *J. Phys. Chem*. **1980**, *84*, 1822. (b) Cherian, S.; Wamser, C. C. *J. Phys. Chem. B* **1999**, *104*, 3624. (c) Fungo, F.; Otero, L.; Durantini, E. N.; Silber, J. J.; Sereno, L. E. *J. Phys. Chem. B* **2000**, *104*, 7644.

(39) (a) Yamada, K.; Imahori, H.; Nishimura, Y.; Yamazaki, I.; Sakata, Y. *Chem. Lett.* **1999**, 895. (b) Tamaki, K.; Imahori, H.; Nishimura, Y.; Yamazaki, I.; Sakata, Y. *Chem. Commun.* **1999**, 625. (c) Luo, C.; Guldi, D. M.; Imahori, H.; Tamaki, K.; Sakata, Y. *J. Am. Chem. Soc.* **2000**, *122*, 6535.